Decentralized Relative Navigation for Formation Flying Spacecraft using Augmented CDGPS [1]

Chan-Woo Park, Philip Ferguson, Nick Pohlman, Jonathan P. How

Massachusetts Institute of Technology

BIOGRAPHY

Chan-Woo Park is a Postdoctoral Associate in the Dept. of Aeronautics and Astronautics at MIT. He received his BS from Seoul National University and MS and Ph.D. in the Dept. of Mechanical Engineering from Stanford University. His research involves the use of GPS for autonomous navigation.

Philip Ferguson is a Research Assistant in the Dept. of Aeronautics and Astronautics at MIT. He received his B.A.Sc from the University of Toronto. While studying in Toronto, he worked for MDRobotics, developing the robots for the International Space Station. His research involves the distributed control architectures for space applications.

Nick Pohlman is a Research Assistant in the Dept. of Aeronautics and Astronautics at MIT. He received his BS from the University of Dayton. His research involves the use of GPS as a sensor for multiple vehicle coordination and control.

Jonathan How is an Associate Professor in the Dept. of Aeronautics and Astronautics at MIT. He received his B.A.Sc (1987) from the University of Toronto, and SM (1990) and Ph.D. (1993) from MIT, both in the Dept. of Aeronautics and Astronautics. His research involves the use of GPS for autonomous navigation and control.

ABSTRACT

Autonomous formation flying of multiple vehicles is a key technology for both deep space and orbital applications that involve multiple spacecraft. Many future space applications will benefit from using formation flying technologies to perform distributed observations (*e.g.,* synthetic apertures radars and stellar interferometry) and to provide improved coverage for communication and surveillance. One of the key requirements of formation flying is accurate real-time knowledge of the relative positions and velocities between the vehicles. Several researchers have shown that carrier-phase differential Global Positioning System (CDGPS) is a viable sensor to perform this relative navigation. This paper extends the previous work by presenting a decentralized algorithm for this CDGPS relative navigation, without degrading the estimation performance. Furthermore, it is shown that a decentralized implementation adds robustness and improves mission flexibility. The paper also considers spacecraft formations that have local RF ranging devices onboard the vehicles, which was recently proposed to overcome possible limitations associated with a NAVSTAR-only relative navigation sensor (limited availability and accuracy). These additional RF measurements couple the states in the system, thus rendering the previous decentralization scheme inapplicable. This problem is addressed by using an approximate decentralized approach, called *Iterative Cascade Extended Kalman Filter* (ICEKF). This new estimation approach is compared to a centralized estimation scheme using a typical LEO simulation. The results clearly show that the decentralized ICEKF approach substantially reduces the computational load, eliminates many of the implementation problems associated with the centralized algorithm, and reduces the communication requirements amongst the vehicles in the fleet.

1 INTRODUCTION

The concept of autonomous formation flying of satellite clusters has been identified as an enabling technology for many future NASA and U.S. Air Force missions [1, 2, 3, 4] (*e.g.* sparse aperture radar, earth mapping, and stellar interferometry). This novel concept is based on the idea that a monolithic spacecraft can be distributed into several small, inexpensive vehicles that collectively form a virtual spacecraft bus of unlimited scale, resulting in a significant improvement in the mission capability and flexibility. For example, a separated interferometer can be formed in space that has a baseline of several kilometers, which would be impractical to build using existing technologies. Another example is the separated spacecraft synthetic aperture radar (SAR) that could obtain an extremely high resolution using distributed and coordinated measurements from multiple apertures onboard formation flying spacecraft.

[1] Presented at the Institute of Navigation *GPS 2001* September 2001.

The ability to accurately and robustly measure (in real-time) the relative position and velocity between all the vehicles in the formation is vital to successfully accomplish the formation flying missions. This level of accuracy will determine the navigation precision of the formation, which is a determining factor for most science missions. Several researchers have shown that GPS is an accurate relative navigation and attitude sensor [5, 6, 13, 14, 15]. In particular, differential carrier-phase measurements of GPS (CDGPS) can provide centimeter-level relative position between the vehicles the fleet. However, several proposed formation flying missions require even tighter precision in environments that are poorly served by the NAVSTAR constellation. Thus it will be hard to meet all of the requirements with a GPS-only navigation system. In this case, an alternative approach is to equip the vehicles in the formation with onboard devices that transmit RF ranging signals. This array of transmitters created by the cluster of vehicles can form a local constellation that augments the NAVSTAR constellation. By providing additional local range and Doppler measurements to the navigation solution, these onboard transmitters can assist the use of CDGPS for many mission scenarios even if adequate visibility/geometry to the NAVSTAR constellation is not available [19] (for example, MEO and GEO formation flying missions). These RF ranging devices can be designed [16, 17, 18] to provide far more accurate measurements of the vehicle relative ranges and range rates than the traditional GPS pseudolites [24]. These more accurate measurements can be combined with the CDGPS to provide improved geometry/availability, thereby resulting in much better overall estimates of the vehicle relative positions and velocities.

While augmented CDGPS can provide the relative navigation performance required for many future missions, several computational and communication issues must be addressed for large fleets of vehicles. These issues arise because the computational and communication requirements of a centralized estimator grow rapidly with the size of the fleet (n). However, many of these difficulties could be overcome by developing a decentralized estimation approach for this system. Standard advantages of decentralized systems include modularity, robustness, flexibility, and extensibility [23]. Note that these advantages are typically achieved at the expense of degraded performance (due to constraints imposed on the solution algorithms) and an increase in the communication requirements because the processing units must exchange information [23]. However, the results in this paper show that the standard CDGPS estimation process naturally decentralizes and can be distributed amongst the multiple vehicles in the fleet, with no loss in performance. The GPS information in this new approach is processed locally on each vehicle, so there is no "master" vehicle. Thus the approach recovers the standard advantages of decentralization cited previously (robustness and flexibility). Furthermore, it is also shown that this decentralized approach actually has substantially lower processing and communication requirements when compared to an equivalent centralized algorithm. This breakthrough is accomplished by using the decoupled nature of the formation flying measurement structure, which appears to have been overlooked in previous distributed implementations [14].

A completely decoupled set of estimation problems can be formulated for the NAVSTAR-only systems because the members in the formation do not impact the observations/measurements of the other vehicles. However, in the *augmented* GPS system, the inter-vehicle measurements must be processed in addition to the NAVSTAR measurements. In this case, the measurement model is nonlinear and depends on the states of all vehicles in the fleet. This paper presents approximate decentralized relative position and velocity estimation algorithms for formation flying vehicles that address these issues for fleets that use augmented CDGPS sensors. These algorithms are also shown to recover the benefits of decentralization, yield near-optimal performance, and greatly reduce the computation and communication requirements for the fleet.

2 FORMATION MEASUREMENT EQUATION

2.1 Measurement Equations Using NAVSTAR Satellites

For the formation flying applications of interest in this paper, estimation of relative position and velocity is performed using measurements from both the NAVSTAR satellites and onboard transmitters (pseudolites). Attaching the formation coordinate system to a *master* vehicle (designated as vehicle m), the measurements from the NAVSTAR constellation can then be written in vector form [5, 6] as

$$\Delta\phi^s{}_{mi} = G_m \begin{bmatrix} X_i \\ \tau_i \end{bmatrix} + \beta^s{}_{mi} + \nu^s{}_{mi} \qquad (1)$$

where

$\Delta\phi^s{}_{mi}$ = differential carrier phase between vehicles m and i using the NAVSTAR signals

$$G_i = \begin{bmatrix} los_i^1 & 1 \\ los_i^2 & 1 \\ \vdots & \vdots \\ los_i^n & 1 \end{bmatrix}$$

X_i = position of vehicle i relative to vehicle m

τ_i = relative clock bias between receivers on vehicles m and i

${\beta^s}_{mi}$ = carrier-phase biases for the single-differences

${\nu^s}_{mi}$ = carrier-phase noise of the NAVSTAR signals

R_i is a diagonal matrix where the diagonal elements are the ranges from i^{th} vehicle to the NAVSTAR satellites $1, 2, \ldots, n$. G_i is the traditional geometry matrix. The components los_i^k are the line-of-sights from the i^{th} user vehicle to the k^{th} NAVSTAR satellite in the formation coordinate frame.

For an N-vehicle formation, these measurements are combined into one equation

$$\begin{aligned}\Delta\Phi^s &= \begin{bmatrix} G_m & & & 0 \\ & G_m & & \\ & & \ddots & \\ 0 & & & G_m \end{bmatrix} \begin{bmatrix} X_1 \\ \tau_1 \\ \vdots \\ X_{N-1} \\ \tau_{N-1} \end{bmatrix} \\ &\quad + \begin{bmatrix} {\beta^s}_{m1} \\ {\beta^s}_{m2} \\ \vdots \\ {\beta^s}_{mN-1} \end{bmatrix} + \nu^s \qquad (2) \\ &= GX + \beta^s + \nu^s \qquad (3)\end{aligned}$$

where

$$\Delta\Phi^s = \begin{bmatrix} {\Delta\phi^s}_{m1} \\ {\Delta\phi^s}_{m2} \\ \vdots \\ {\Delta\phi^s}_{mN-1} \end{bmatrix}$$

and it is assumed that the *master* vehicle m had visibility to all available satellites and all the vehicles track the same set of satellites. In general this may not be the case, and G may have off-diagonal terms corresponding to the single differences that can be made between vehicles using NAVSTAR signals not available on the *master* vehicle. In addition, not all of the block diagonal entries will be G_m as shown in Eq. 2. For example, if the k^{th} GPS satellite was not visible on vehicle m, but was visible on vehicles i and j, then the following single difference could be formed

$$\Delta\phi_{ji} + R_j^k(1 - los_i^k \cdot los_j^k) = los_i^k(X_j - X_i) + \tau_j - \tau_i + \beta_{ij}^s + \nu_{ij}^s \qquad (4)$$

where R_j^k is the range from the j^{th} vehicle to the k^{th} GPS satellite. This measurement would be added to those using the *master* vehicle, and would appear in the off-diagonal elements of G.

Doppler measurements using n NAVSTAR satellite signals can also be represented in vector form. When differential Doppler measurements are formed between the *master* vehicle and vehicle i,

$$\Delta\dot{\phi}_{mi}^s = G_i \begin{bmatrix} \dot{X}_i \\ \dot{\tau}_i \end{bmatrix} + \dot{\nu}_{mi}^s \qquad (5)$$

where

$\Delta\dot{\phi}_{mi}^s$ = differential carrier phase Doppler between vehicles m and i using the NAVSTAR signals

$\dot{X}_i$ = velocity of vehicle i relative to vehicle m

$\dot{\tau}_i$ = relative clock drift rate between receivers on vehicles m and i

$\dot{\nu}_{mi}^s$ = carrier-phase Doppler noise for the single-differences between vehicles m and i using the NAVSTAR signals

For an N-vehicle formation, these measurements are combined into one equation

$$\begin{aligned}\Delta\dot{\Phi}^s &= \begin{bmatrix} G_1 & & & 0 \\ & G_2 & & \\ & & \ddots & \\ 0 & & & G_{N-1} \end{bmatrix} \begin{bmatrix} \dot{X}_1 \\ \dot{\tau}_1 \\ \vdots \\ \dot{X}_{N-1} \\ \dot{\tau}_{N-1} \end{bmatrix} + \dot{\nu}^s \\ &= G_v\dot{X} + \dot{\nu}^s \qquad (6)\end{aligned}$$

where

$$\Delta\dot{\Phi}^s = \begin{bmatrix} \Delta\dot{\phi}_{m1}^s \\ \Delta\dot{\phi}_{m2}^s \\ \vdots \\ \Delta\dot{\phi}_{mN-1}^s \end{bmatrix}$$

As in the position equation, it is assumed that *master* vehicle m has visibility to all available satellites and all of the vehicles track the same set of satellites. In general, this may not be the case, especially if the separation between the spacecraft is large, and G_v may also have off-diagonal terms corresponding to the single differences that can be made between vehicles using NAVSTAR signals not available on the *master* vehicle. For example, if the k^{th} GPS satellite was not visible on vehicle m, but was visible on vehicles i and j, then the following Doppler single difference could be formed

$$\begin{aligned}\Delta\dot{\phi}_{ij} &+ (los_j^k - los_i^k)(V_i - V_{SV}^k) \\ &= los_j^k\dot{X}_{ij} + \dot{\tau}_{ij} + \dot{\nu}_{ij}^s \qquad (7) \\ \dot{X}_{ij} &= \dot{X}_j - \dot{X}_i \qquad (8)\end{aligned}$$

This measurement would be added to those using the *master* vehicle and would appear in the off-diagonal elements of G_v.

These two velocity and position equations for formation vehicles can also be combined into a single matrix equation

$$\begin{bmatrix} \Delta\Phi^s \\ \Delta\dot{\Phi}^s \end{bmatrix} = \begin{bmatrix} G & 0 \\ 0 & G_v \end{bmatrix} \begin{bmatrix} X \\ \dot{X} \end{bmatrix} + \begin{bmatrix} \beta^s \\ 0 \end{bmatrix} + \begin{bmatrix} \nu^s \\ \dot{\nu}^s \end{bmatrix} \qquad (9)$$

2.2 Measurement Equation Using Local Transmitters

In addition to the signals generated by the NAVSTAR constellation, each vehicle in the formation could have onboard transmitters or ranging devices that provide additional measurements. Because the local transmitters are very close, the full nonlinear measurements equations must be used. The transmitter on vehicle m can be used to form ranging measurements that are given by

$$\Delta\phi^p{}_{mi} = d_{mi}(X_i) + \tau_i + \beta^p{}_{mi} + \nu^p{}_{mi} \qquad (10)$$

where

$\Delta\phi^p{}_{mi}$ = differential carrier phase between vehicles m and i using signal generated on vehicle m

$d_{mi}(X_i)$ = distance between vehicles m and i

τ_i = relative clock bias (in meters) between receivers on vehicles m and i,

$\beta^p{}_{mi}$ = carrier-phase biases for the single-difference between vehicles m and i using the transmitter on vehicle m

$\nu^p{}_{mi}$ = carrier-phase noise for the single-difference between vehicles m and i using the transmitter on vehicle m

The signal generated on vehicle m is assumed to have been measured on the vehicle itself. This can be accomplished by running the signal through a splitter to both the transmit antenna and the receiver. Alternatively, the receiver antenna that receives the NAVSTAR signals and/or the ranging signals from other vehicles can be used to track the signal transmitted by itself if the antennas are oriented properly. The single difference formed between vehicles i and m, using the transmitter on vehicle i can be written as

$$\Delta\phi^p{}_{im} = d_{im}(X_i) - \tau_i + \beta^p{}_{im} + \nu^p{}_{im} \qquad (11)$$

Additionally, measurements can be formed between vehicles i and j (using the transmitter on vehicle i), exclusive of vehicle m. These are written as

$$\Delta\phi^p{}_{ij} = d_{ij}(X_i, X_j) + \tau_j - \tau_i + \beta^p{}_{ij} + \nu^p{}_{ij} \qquad (12)$$

In this case, the range and relative clock biases between the two vehicles are written in terms of their positions and the clock biases relative to vehicle m. The single difference made using the transmitter on vehicle j is derived by interchanging the indexes in Eq. 12. These differences are formed between all of the vehicles in the system in order to generate a maximal set of independent measurements. Note that for an N-vehicle formation, there are a total of $N \times (N-1)$ independent inter-vehicle single differences that can be formed. If double differences were used, there would be a total of $N \times (N-1)/2$ independent measurements with out the clock bias terms.

In addition, Doppler measurements from the local transmitters can be included in the relative velocity measurement equation. For the transmitter on vehicle m,

$$\Delta\dot{\phi}^p_{mi} = \dot{d}_{mi}(X_i) + \dot{\tau}_i + \dot{\nu}^p_{mi} \qquad (13)$$

$$= \frac{X_i}{d_{mi}(X_i)}\dot{X}_i + \dot{\tau}_i + \dot{\nu}^p_{mi} \qquad (14)$$

where

$\Delta\dot{\phi}^p_{mi}$ = differential carrier Doppler between vehicles m and i using the signal generated on vehicle m

$\dot{d}_{mi}(X_i)$ = range rate between vehicles m and i

$\dot{\tau}_i$ = relative clock drift (in m/sec) between the receivers on vehicles m and i,

$\dot{\nu}^p_{mi}$ = carrier Doppler noise for the single-difference between vehicles m and i using the transmitter on vehicle m

Similar to the discussion above, measurements can be formed using the signal transmitted from vehicle i and differential measurements can be formed between vehicles i and j, exclusive of vehicle m.

The following sections discuss how these measurement equations are used to solve for the formation state (relative position and velocities) and carrier phase ambiguities.

3 STATE ESTIMATION

This section outlines the general state estimation methods. A weighted least squares method is used for the state estimation problem if a dynamic model of the vehicle is not available. A dynamic model can be used within an extended Kalman filter. The measurements from NAVSTAR satellites and the local transmitters can be combined to form a single weighted least squares (WLS) equation. Since the measurements from the local transmitter signals are nonlinear, the combined nonlinear measurement equation can be expressed as

$$\begin{bmatrix} \Delta\Phi^s \\ \Delta\dot{\Phi}^s \\ \Delta\Phi^p \\ \Delta\dot{\Phi}^p \end{bmatrix} = h\left(\begin{bmatrix} X \\ \dot{X} \end{bmatrix}\right) + \begin{bmatrix} \beta^s \\ 0 \\ \beta^p \\ 0 \end{bmatrix} + \begin{bmatrix} \nu^s \\ \dot{\nu}^s \\ \nu^p \\ \dot{\nu}^p \end{bmatrix} \qquad (15)$$

This equation can be linearized about the current estimate of the position and velocity states

$$\begin{bmatrix} \delta\Delta\Phi^s \\ \delta\Delta\dot{\Phi}^s \\ \delta\Delta\Phi^p \\ \delta\Delta\dot{\Phi}^p \end{bmatrix} = \begin{bmatrix} G & 0 \\ 0 & G_v \\ \frac{\partial D(X)}{\partial X}\Big|_{\hat{X}} & 0 \\ \frac{\partial \dot{D}(X)}{\partial X}\Big|_{\hat{X}} & \frac{\partial \dot{D}(X)}{\partial \dot{X}}\Big|_{\hat{\dot{X}}} \end{bmatrix} \begin{bmatrix} \delta X \\ \delta \dot{X} \end{bmatrix} + \begin{bmatrix} \beta^s \\ 0 \\ \beta^p \\ 0 \end{bmatrix} + \begin{bmatrix} \nu^s \\ \dot{\nu}^s \\ \nu^p \\ \dot{\nu}^p \end{bmatrix} \quad (16)$$

where

$$h\left(\begin{bmatrix} X \\ \dot{X} \end{bmatrix}\right) = \begin{bmatrix} GX \\ G_v\dot{X} \\ D(X) \\ \dot{D}(X) \end{bmatrix}$$

$$D(X) = \begin{bmatrix} d_{m1}(X_1) \\ d_{m2}(X_2) \\ \vdots \\ d_{N-2,N-1}(X_{N-1}, X_{N-2}) \end{bmatrix}$$

are the $\frac{N(N-1)}{2}$local range measurements

$$\dot{D}(X) = \begin{bmatrix} \dot{d}_{m1}(X_1) \\ \dot{d}_{m2}(X_2) \\ \vdots \\ \dot{d}_{N-2,N-1}(X_{N-2}, X_{N-1}) \end{bmatrix}$$

are the $\frac{N(N-1)}{2}$ local Doppler measurements

and $\delta\Delta\Phi^s = \Delta\Phi^s - G\hat{X}$, $\delta\Delta\Phi^p = \Delta\Phi^p - D(\hat{X})$.

With a prior estimate of the bias states $\hat{\beta}^s$ and $\hat{\beta}^p$, the position and velocity states could be updated using a standard WLS approach

$$\begin{bmatrix} \delta X \\ \delta \dot{X} \end{bmatrix} = (H^T W H)^{-1} H^T W \left(\begin{bmatrix} \delta\Delta\Phi^s \\ \delta\Delta\dot{\Phi}^s \\ \delta\Delta\Phi^p \\ \delta\Delta\dot{\Phi}^p \end{bmatrix} - \begin{bmatrix} \hat{\beta}^s \\ 0 \\ \hat{\beta}^p \\ 0 \end{bmatrix} \right) \quad (17)$$

where H is block measurement matrix in the Eq. 16 and W is the weighting matrix.

$$H = \begin{bmatrix} G & 0 \\ 0 & G_v \\ \frac{\partial D(X)}{\partial X}\Big|_{\hat{X}} & 0 \\ \frac{\partial \dot{D}(X)}{\partial X}\Big|_{\hat{X}} & \frac{\partial \dot{D}(X)}{\partial \dot{X}}\Big|_{\hat{\dot{X}}} \end{bmatrix} \quad (18)$$

The position and velocity states can then be updated as,

$$\begin{bmatrix} \hat{X} \\ \hat{\dot{X}} \end{bmatrix}^+ = \begin{bmatrix} \hat{X} \\ \hat{\dot{X}} \end{bmatrix}^- + \begin{bmatrix} \delta X \\ \delta \dot{X} \end{bmatrix} \quad (19)$$

The position state $\hat{X}$ and velocity state $\dot{\hat{X}}$ can be updated each time that new measurements are available or when the bias state has been updated using the approach described below. Note that the position and velocity states are coupled in the local transmitter measurements, which differs from the general CDGPS position/velocity estimation schemes. Further improvement can be achieved in the position and velocity estimate accuracy by incorporating the relative dynamics of the vehicle into the filter. Typically, a nonlinear dynamic model (Eq. 20) of the vehicle can be included in the extended Kalman filter formulation.

$$\begin{bmatrix} \dot{X} \\ \ddot{X} \end{bmatrix} = \mathcal{F}^c\left(\begin{bmatrix} X \\ \dot{X} \end{bmatrix}, \mathbf{u}, \mathbf{w}\right) \quad (20)$$

where $\mathbf{u}$ and $\mathbf{w}$ are the control input and the disturbance to the model. The discrete dynamic model and the process noise covariance matrix are derived in the Appendix 5. To simplify the following discussion, define

$$\chi_n = \begin{bmatrix} X \\ \dot{X} \end{bmatrix}_n \quad (21)$$

In order to use the extended Kalman filter algorithm, the nonlinear discrete propagation model $\mathcal{F}_n^d(\chi)$ should be linearized about the current estimate $\hat{\chi}_{n|n}$

$$F_n = \frac{\partial \mathcal{F}_n^d(\chi)}{\partial \chi}\Big|_{\chi=\hat{\chi}_{n|n}} \quad (22)$$

With the estimate of current state $\hat{\chi}_{n|n}$, Eq. 41 can be approximated as

$$\chi_{n+1} = \mathcal{F}_n^d(\hat{\chi}_{n|n}) + F_n(\chi_n - \hat{\chi}_{n|n}) + G_n\mathbf{w}_n \quad (23)$$

$$= F_n\chi_n + \underbrace{\mathcal{F}_n^d(\hat{\chi}_{n|n}) - F_n\hat{\chi}_{n|n}}_{\text{known}} + G_n\mathbf{w}_n \quad (24)$$

which is a linear propagation model for χ_n. Applying the Kalman filter equations [10, 9, 12],

$$\hat{\chi}_{n+1|n} = F_n\hat{\chi}_{n|n} + \mathcal{F}_n^d(\hat{\chi}_{n|n}) - F_n\hat{\chi}_{n|n} \quad (25)$$

$$= \mathcal{F}_n^d(\hat{\chi}_{n|n}) \quad (26)$$

The EKF time update equations can be written as

$$\hat{\chi}_{n+1|n} = \mathcal{F}_n^d(\hat{\chi}_{n|n}) \quad (27)$$

$$P_{n+1|n} = F_nP_{n|n}F_n^T + G_nQ_nG_n^T \quad (28)$$

The last term in Eq. 28 can be calculated from the continuous process noise covariance matrix Q using Eqs. 44 and 45.

The measurement update equations can be derived from Eq. 15 (Note that the measurement equation is also nonlinear). Define

$$y_n = \begin{bmatrix} \Delta\Phi^s \\ \Delta\dot{\Phi}^s \\ \Delta\Phi^p \\ \Delta\dot{\Phi}^p \end{bmatrix}_n, \ \bar{\beta} = \begin{bmatrix} \beta^s \\ 0 \\ \beta^p \\ 0 \end{bmatrix}, \ \bar{\nu}_n = \begin{bmatrix} \nu^s \\ \dot{\nu}^s \\ \nu^p \\ \dot{\nu}^p \end{bmatrix}_n \quad (29)$$

Rewriting Eq. 15 with these new definitions,

$$y_n = h(\chi_n) + \bar{\beta} + \bar{\nu} \quad (30)$$

$$H_n = \left.\frac{\partial h(\chi)}{\partial \chi}\right|_{\chi=\hat{\chi}_{n|n-1}} \quad (31)$$

The EKF measurement update equations are

$$\hat{\chi}_{n|n} = \hat{\chi}_{n|n-1} + K_n\left[y_n - \hat{\bar{\beta}}_{n|n} - h_n(\hat{\chi}_{n|n-1})\right] \quad (32)$$

$$K_n = P_{n|n-1}H_n^T\left(H_n P_{n|n-1} H_n^T + R_n\right)^{-1} \quad (33)$$

$$P_{n|n} = \left(I - K_n H_n\right) P_{n|n-1} \quad (34)$$

where R_n is the covariance matrix of the discrete white sensing noise.

$$R_i\delta_{ij} = E[\bar{\nu}_i\bar{\nu}_j^T] \quad (35)$$

4 DECENTRALIZED ITERATIVE CASCADE EKF

This section analyzes the numerical, computational, and implementation issues in the EKF state estimation problem for a fleet of vehicles. Note that, building on the work of [22, 23] Ref. [14] developed a decentralized approach for the spacecraft formation flying problem using a GPS sensor. However, the work of [14] does not take full advantage of the decoupled observation structure in the differential GPS sensing system. By taking this structure into account, this section presents a simple and efficient decentralized approach to the formation estimation problem.

4.1 NAVSTAR-only Navigation System

The sparse nature of the observation matrix H in Eq. 16 provides the basis for developing the decentralized estimation algorithm, which reduces the processing time and yields better numerical stability. The observation matrix H in Eq. 16 is completely block diagonal without the local range and range rate measurements (NAVSTAR-only system) if the master vehicle has visibility to all NAVSTAR satellites visible to the entire formation. This would be the normal case for a closely spaced fleet of spacecraft in LEO, if the spacecraft carry more than one antenna.[1] In this case, Eq. 16 can be divided into $N-1$ independent (and small) estimation filters (N is the number of vehicles) for each vehicle state relative to the master vehicle. These estimation problems can then be easily distributed amongst the vehicles in the formation. This simple, straightforward distribution is possible because the relative dynamic models are also almost completely decoupled. The process is illustrated in Figure 1.

[1] Multiple antennas mounted on a spacecraft facing in different directions dramatically increase sky coverage [21, 20].

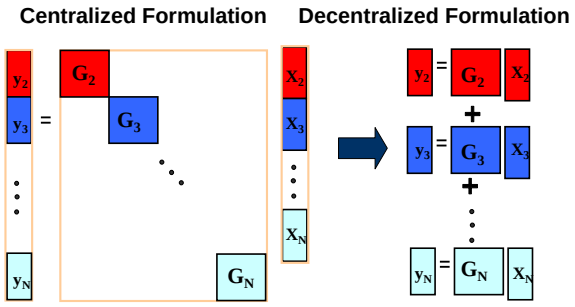

Fig. 1: Centralized Formulation and Decentralized Formulation

This distribution of effort greatly reduces the computational load for the NAVSTAR-only system, especially when the formation is quite large. As a result, the computational load *per* vehicle in the decentralized system is significantly lower than that of the centralized system and independent of the number of vehicles in the fleet. Note that, since the measurement matrix decouples naturally, there is no degradation in the estimation performance as a result of this decentralization.

The decentralized approach also provides a robust and flexible architecture that is less sensitive to a single vehicle failure. For example, with a centralized solution approach, the *master* vehicle performs most of the calculations for the fleet, therefore, unless all vehicles are designed with the same processor as the master vehicle, the entire system could be susceptible to a single point failure. However, in the decentralized approach, all that is required is that one spacecraft act as the *reference* vehicle which serves as the center of the formation reference frame. The estimation process is then evenly distributed amongst the vehicles in the fleet. As such, the vehicles could be designed to be identical in terms of their computational capability – and the CPU's could be much simpler. Note that if one vehicle failed, switching the *reference* vehicle from one spacecraft to another would be a much simpler task than switching the *master* vehicle of the centralized approach. The results in the following sections also show that, when compared to a centralized estimation scheme, the decentralized CDGPS estimation process actually reduces the communication requirements between the vehicles.

4.2 Systems with Local Range Measurements: Iterative Cascade EKF

Section 4.1 discussed the advantages of distributing the estimation, and it would be very beneficial to perform the same process when the local ranging devices are available to augment the NAVSTAR measurements. However, the local transmitter measurements from non-

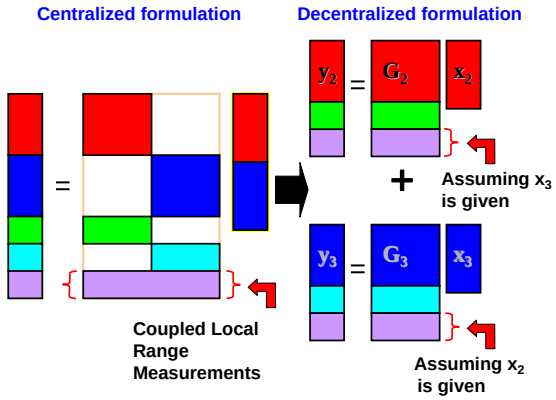

Fig. 2: Coupled Measurement Equation and Multiple Decoupled Equations of Augmented NAVSTAR System. Compare to decoupled equations of NAVSTAR-only system in Fig. 1)

master vehicles are coupled across the vehicles, and they appear as off-diagonal terms in the linearized measurement matrix. As will be shown, it is important to keep all local range measurements to obtain the best possible estimate, but these off-diagonal measurements complicate the process of distributing the estimation. However, it is possible to develop an approximate decentralized estimation architecture using the following iterative scheme.

The left hand side diagram in Figure 2 is a schematic of the linearized measurement equation for a 3-vehicle formation combining all the measurements available in the system. As shown, this equation can be divided into multiple smaller problems. The coupled local measurements, which are a function of more than one vehicle state, can also be divided using an approximation. In particular, it is assumed that the states for all the other vehicles (X_k, $\{\ k = 1, 2, \ldots, N-1 \mid k \neq i\ \}$) are available for the i^{th} divided estimation process ($i = 1, 2, \ldots, N-1$). This decentralization process can be explained in detail by rearranging the previous measurement equations. Instead of stacking all the measurements for all the vehicle, as in Eqs. 6 and 2, the measurements for a single vehicle are combined with the local measurements available to that vehicle. For the i^{th} vehicle

$$\begin{bmatrix} \Delta\phi^s_{mi} \\ \Delta\dot{\phi}^s_{mi} \\ \Delta\phi^p_i \\ \Delta\dot{\phi}^p_i \end{bmatrix} = h\left(\begin{bmatrix} X \\ \dot{X} \end{bmatrix}\right) + \begin{bmatrix} \beta^s_{mi} \\ 0 \\ \beta^p_i \\ 0 \end{bmatrix} + \begin{bmatrix} \nu^s_{mi} \\ \dot{\nu}^s_{mi} \\ \nu^p_i \\ \dot{\nu}^p_i \end{bmatrix} \quad (36)$$

where

$$h\left(\begin{bmatrix} X \\ \dot{X} \end{bmatrix}\right) = \begin{bmatrix} G_m \begin{bmatrix} X_i \\ \tau_i \end{bmatrix} \\ G_i \begin{bmatrix} \dot{X}_i \\ \dot{\tau}_i \end{bmatrix} \\ D_i(X) \\ \dot{D}_i(X) \end{bmatrix}$$

$D_i(X)$ = ranges between vehicle i and all other vehicles

$\dot{D}_i(X)$ = range rates between vehicle i and all other vehicles

$\Delta\phi^p_i$ = local range measurements between vehicle i and all other vehicles

$\Delta\dot{\phi}^p_i$ = local Doppler measurements between vehicle i and all other vehicles

The equation for i^{th} vehicle can be linearized about the best current estimate of the position and velocity states of other vehicles X_k and $\dot{X}_k$ $\{k = 1, 2, \ldots, N-1 \mid k \neq i\}$

$$\begin{bmatrix} \delta\Delta\phi^s_{mi} \\ \delta\Delta\dot{\phi}^s_{mi} \\ \delta\Delta\phi^p_i \\ \delta\Delta\dot{\phi}^p_i \end{bmatrix} = \begin{bmatrix} G_m & 0 \\ 0 & G_i \\ \frac{\partial D_i(X)}{\partial X_i}\Big|_{\hat{X}_i} & 0 \\ \frac{\partial \dot{D}_i(X)}{\partial X_i}\Big|_{\hat{X}_i} & \frac{\partial \dot{D}_i(X)}{\partial \dot{X}}\Big|_{\hat{\dot{X}}_i} \end{bmatrix} \begin{bmatrix} \delta X_i \\ \tau_i \\ \delta\dot{X}_i \\ \dot{\tau}_i \end{bmatrix} + \begin{bmatrix} \beta^s_{mi} \\ 0 \\ \beta^p_i \\ 0 \end{bmatrix} + \begin{bmatrix} \nu^s_{mi} \\ \dot{\nu}^s_{mi} \\ \nu^p_i \\ \dot{\nu}^p_i \end{bmatrix} \quad (37)$$

Eq. 37 can be written in simple form for the n^{th} measurement update step.

$$\delta\Delta\Phi_{n,i} = H_{n,i}\ \chi_{n,i} + \beta_i + \nu_i \quad (38)$$

Note that Eq. 37 is the measurement equation for the i^{th} vehicle, so there are only $N-1$ local range measurements. Whenever there are new measurements available, the position and velocity states for vehicles $i = 1, 2, \ldots, N-1$ can be updated sequentially using Eq. 37. After the i^{th} vehicle update, the new estimates of X_i and $\dot{X}_i$ are available to be used in the next sequence where states for $(i+1)^{\text{th}}$ vehicle are updated. After updating states X_i and $\dot{X}_i$ for $i = 1, 2, \ldots, N-1$, an iteration can be performed until updates to the states are very small[2]. The iteration is necessary because the linearization process for the i^{th} vehicle in Eq. 37 not only requires the estimate of state X_i and $\dot{X}_i$ but also the estimated states of all the vehicles in the system X_k's and $\dot{X}_k$'s ($k = 1, 2, \ldots, N-1$).

[2]Experience from numerous simulation indicates that this process typically converges after 3–4 iterations.

In this sequential update scheme, the massive covariance matrix $P_{n|n-1}$ in Eq. 34 can be replaced by $N-1$ smaller covariance matrices corresponding to the states of each vehicle. By updating multiple small covariance matrices ($P_{n|n,i}$) instead of the large covariance matrix ($P_{n|n-1}$), the amount of computation can be reduced and in addition, the reduced computational load can be distributed. Thus, for $i = 1, 2, \ldots, N$-1,

$$P_{n|n,i} = (I - K_{n,i}H_{n,i})P_{n|n-1,i} \tag{39}$$

$P_{n|n-1,i}$ = covariance matrix for the i^{th} vehicle
$K_{n,i}$ = Kalman gain for the i^{th} vehicle
$H_{n,i}$ = linearized measurement matrix for the i^{th} vehicle in Eq. 37

Algorithm #1 summarizes the ICEKF algorithm in pseudo-code form and Figure 3 describes this process for a 4-vehicle formation. The arrows in this figure represent the range measurements used in the estimation process. The diagram on the left describes the traditional centralized EKF that simultaneously uses all of the local measurements in one update process. In contrast, the diagram on the right shows the cascade EKF that uses a subset of the local measurements in a sequential fashion. As shown, the update process is split into three steps (vehicle 2 update, followed by the vehicle 3 update, followed by the vehicle 4 update, and then the process is repeated). Only a fraction of the local measurements are used in each step, but all the available measurements are used in the entire process. Because this method exploits the sparse nature of the measurement equations, the total computational load required in the measurement update can be greatly reduced. Moreover, computational load of the ICEKF method can be distributed to the $N-1$ vehicles in the formation since both the measurement update and covariance update process can be divided into $N-1$ small problems. This dramatically reduces the computational requirements of the onboard CPU for each vehicle.

A series of orbit simulations were conducted to demonstrate the computational efficiency of the decentralized ICEKF (Iterative Cascade Extended Kalman Filter). Figure 4 compares the number of floating point operations (FLOPS) needed in the single measurement update for various formation sizes. The results show the total computation required in the centralized EKF, the total computation required in the ICEKF (3 iterations), and the computation required per each vehicle in the decentralized ICEKF (3 iterations). As expected, the centralized EKF requires the largest amount of computation (2–10 times more than the *total* computation required for the ICEKF). The computation required per each vehicle in the decentralized ICEKF method is 1–2 orders of magnitude lower than the total required for the centralized EKF. Figure 5 plots the ratio of the

Algorithm #1: ICEKF algorithm in Pseudo-code Form.

while update to $\hat{\chi}_n >$ tol
  for $i = 1, 2, \ldots, N$-1
    Linearize measurement Eq. 36 for i^{th} vehicle using $\hat{\chi}_n = \begin{bmatrix} \hat{X} \\ \hat{\dot{X}} \end{bmatrix}_n$
    Compute Kalman gain matrix $K_{n,i}$ for i^{th} vehicle
    Update $\hat{\chi}_{n,i}$
    Update $\hat{\chi}_n$
  end
end

for $i = 1, 2, \ldots, N$-1
  Update $P_{n,i}$ using the $K_{n,i}$ and $H_{n,i}$ used in the last state update
end □

FLOPS required for the decentralized ICEKF to the flops required for the centralized EKF. It is shown that the ICEKF method requires only about 5% of the total computation power required in the centralized EKF if there are 6 vehicles in the formation.

$$\text{Ratio} = \frac{F_{\text{ICEKF}}/(N-1)}{F_{\text{EKF}}} \times 100(\%) \tag{40}$$

where

F_{ICEKF} = Total computation required for the ICEKF method
F_{EKF} = Total computation required for the centralized EKF method
N = Number of vehicle in the formation

Performance of the ICEKF

The performance of the ICEKF algorithm in terms of the estimation accuracy is also vital since the algorithm is an approximation. Orbit simulations for a 5–vehicle formation were performed to compare the steady state position errors of ICEKF method with those of the centralized EKF. Figure 6 compares the RMS (Root Mean Square) position errors of 4 different estimation schemes. The first ($-\circ-$) is the extended Kalman filter solution using only the NAVSTAR measurements and the second ($-\square-$) is the EKF solution, but it also uses local range measurements transmitted from the master vehicle (origin of the local coordinate). These two Kalman filters have block diagonal measurement matrices and can be divided into 4 ($N-1$) small problems without using the approximation used in the ICEKF

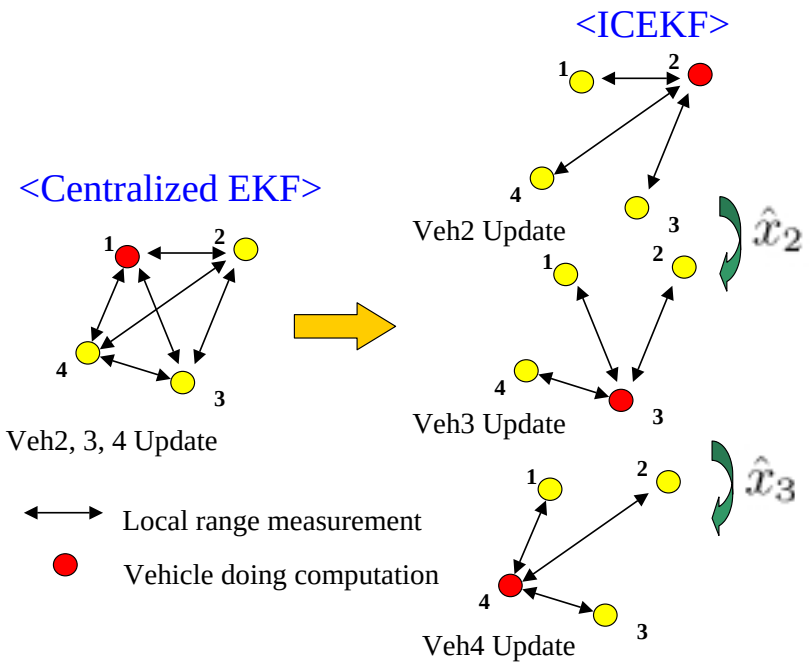

Fig. 3: Full Extended Kalman Filter and Iterative Cascade Kalman Filter (One iteration cycle is shown in the diagram)

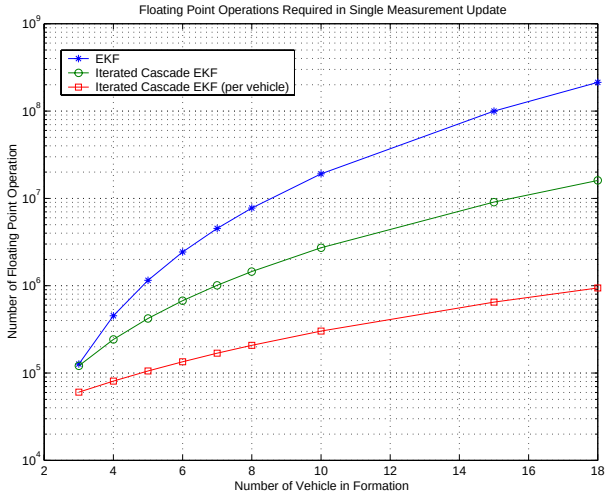

Fig. 4: Computation Required for a Single Update (EKF and ICEKF) - 3 iterations performed in ICEKF

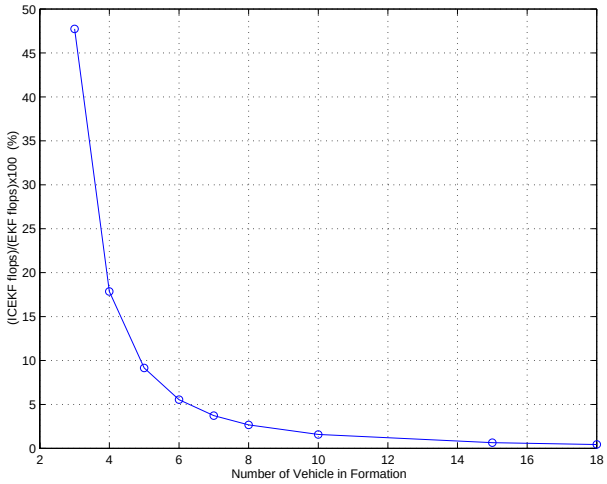

Fig. 5: Ratio of the Computational Power Used (Decentralized ICEKF)/(EKF) (%)

process. However, the second algorithm only uses a subset of the total ranging measurements available to the fleet. In this case, it uses 4 local measurements out of total 10 local measurement available. The third and fourth cases use all of the local range measurements and the NAVSTAR measurements. The centralized EKF ($-\diamond-$) uses all the measurements simultaneously, while the ICEKF ($-\triangle-$) finds the solution iteratively, using all the measurements sequentially in the multiple cascaded EKFs. Comparing cases 1 and 4 in Figure 6 shows the benefits of adding the local measurements. Comparing cases 2 and 4 shows the penalty of ignoring some of the local ranging measurements. Note that improvements achieved by adding more local range measurements are different from vehicle to vehicle. This is because each vehicle in the formation observes different local constellation geometries. Figure 6 also shows that the centralized EKF and the ICEKF using all the local

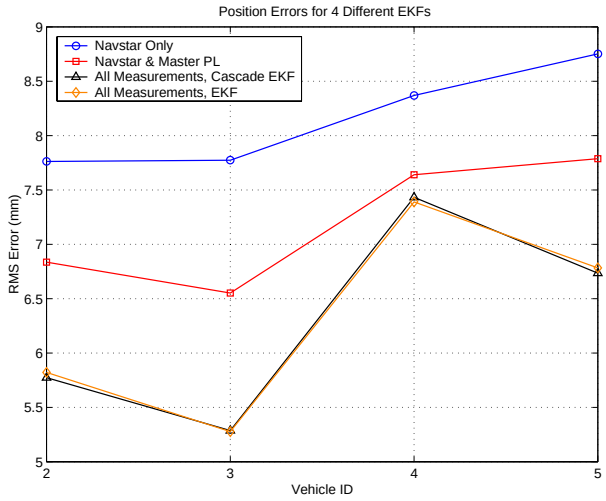

Fig. 6: RMS Position Errors of 4 Different EKFs

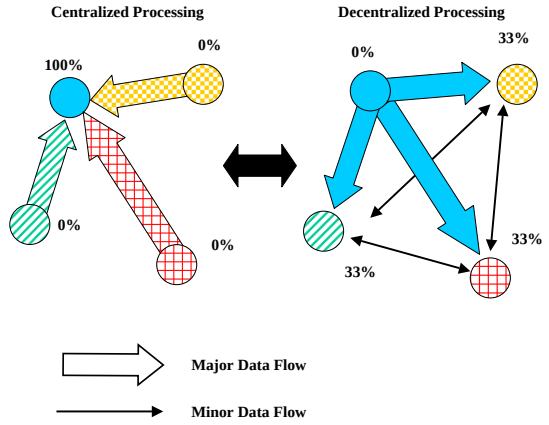

Fig. 7: Information Flows for 2 Architectures

measurements returned essentially an identical answer for relative positions of all the vehicles (vehicle ID = 2, 3, 4, 5). This indicates that the approximations made in the iterative cascade EKF are valid and the ICEKF algorithm can provide near optimal estimates with substantially reduced computational requirements.

Information Flow

In addition to the reduced processing load, another major advantage of this decentralized ICEKF algorithm is that it significantly reduces the inter-vehicle communication requirements. Most formation flying control systems require a communication link between the vehicles in order to exchange data for the relative navigation as well as other operations. Since the bandwidth of the communication link is limited [17], it is highly beneficial to minimize the amount of the navigation data transmitted. Information flow diagrams for the centralized and decentralized systems are conceptually

Table 1: Major Data Packet

	Bytes
Carrier Phase	$4\times n$
Code Phase	$4\times n$
Doppler	$4\times n$
Line-of-sight	$12\times n$
PRN	$1\times n$
Total	$25\times n$

(n= number of NAVSTAR satellites)

Table 2: Minor Data Packet

	Bytes
Local Range	4
Relative Position	12
Total	16

illustrated in Figure 7 for a 4-vehicle formation. The major information includes GPS carrier phase measurements and the line-of-sight matrix, while the minor information includes a single local transmitter measurement and relative position. The centralized estimation method (Left) requires the master vehicle to collect all of the information from all of the vehicles in the formation. This requires a large number of communication channels be available on the master vehicle and an information bottleneck could occur at that point. On the other hand, the decentralized method (Right) allows one vehicle (usually the reference vehicle) to broadcast a data packet. All other vehicles receive this single data packet from the reference vehicle and exchange a few minor pieces of data with the other vehicles. Thus the decentralized architecture has a potential to eliminate the information bottlenecks.

To compare the amount of data exchanged in each method, various data packet sizes for a typical formation system are listed in Table 1 and 2. Based on these examples, the expected maximum data rate requirements are computed for a 1 Hz measurement update. For a N vehicle formation, $N-1$ minor data packets and 1 major data packet are transmitted in the decentralized system. In contrast, $N-1$ major and minor data packets are transmitted in the centralized system. Figure 8 shows the required maximum data rate (bps) for both the centralized and decentralized architectures. As shown, the decentralized system can substantially reduce the amount of data packet transmitted in the system and lower the inter-vehicle communication bandwidth requirements.

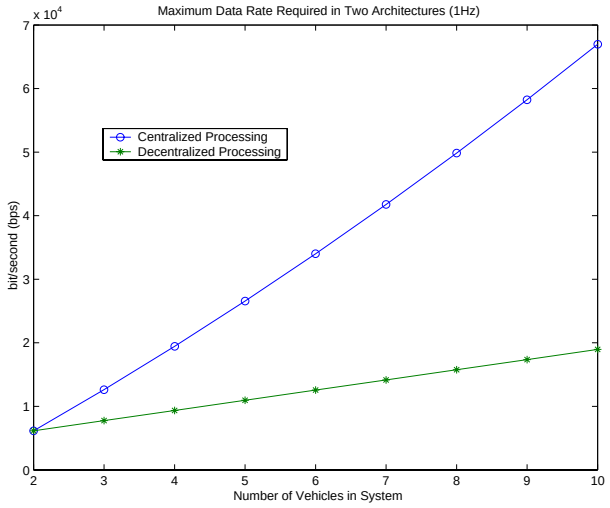

Fig. 8: Maximum Data Rate Required in 2 Communication Architectures

5 CONCLUSIONS

The new efficient decentralized position and velocity estimation algorithm is introduced for the formation flying vehicles using the GPS and the onboard ranging devices. The performance of the decentralized ICEKF algorithm that can be easily distributed to multiple processors is analyzed and compared to the results of the optimal centralized Kalman filter method. In addition, the estimated savings in the inter-vehicle communication requirement that can be achieved in the CDGPS decentralized estimation scheme are shown and compared to that of the centralized system. The numerical problems associated with the centralized system are simulated and the effect of the large number of vehicles in the formation is shown and it is compared to the result of the decentralized system with the same number of vehicles.

ACKNOWLEDGMENTS

This research is funded in part by NASA Grant NAG5-10440.

APPENDIX: NOISE MODELS

A discrete model used in the EKF can be formed from the continuous model (Eq. 20).

$$\begin{bmatrix} X \\ \dot{X} \end{bmatrix}_{n+1} = \mathcal{F}_n^d \left(\begin{bmatrix} X \\ \dot{X} \end{bmatrix}_n \right) + G_n \mathbf{w}_n \qquad (41)$$

Following the standard derivation of the discrete equivalent for the noise covariance matrices [8, 9], we have

$$G_n \simeq G\Delta t \qquad (42)$$

where Δt is assumed to be small.w_n in Eq. 41 is the discrete version of the process noise and the covariance matrix is defined as

$$Q_n \delta_{nm} = E[\mathbf{w}_n \mathbf{w}_m^T] \qquad (43)$$

The discrete process noise covariance matrix Q_n has the following relationship with the continuous counterpart

$$G_n Q_n G_n^T \simeq G Q G^T \Delta t \qquad (44)$$

where $Q\delta(t-\tau) = E\left[w(t)w(t-\tau)^T\right]$ is the spectral density of the white process noise. Using Eq. 42, the covariance matrix Q_n of the discrete white noise can be approximated as

$$Q_n \simeq \frac{Q}{\Delta t} \qquad (45)$$

REFERENCES

[1] F. H. Bauer, J. Bristow, D. Folta, K. Hartman, D. Quinn, J. P. How, "Satellite Formation Flying Using an Innovative Autonomous Control System (AUTOCON) Environment," proceedings of the *AIAA/AAS Astrodynamics Specialists Conference*, New Orleans, LA, August 11-13, 1997, AIAA Paper 97-3821.

[2] F. H. Bauer, K. Hartman, E. G. Lightsey, "Spaceborne GPS: Current Status and Future Visions," proceedings of the *ION-GPS Conference*, Nashville, TN, Sept. 1998, pp. 1493–1508.

[3] F. H. Bauer, K. Hartman, J. P. How, J. Bristow, D. Weidow, and F. Busse, "Enabling Spacecraft Formation Flying through Spaceborne GPS and Enhanced Automation Technologies," proceedings of the *ION-GPS Conference*, Nashville, TN, Sept. 1999, pp. 369–384.

[4] A. Das and R. Cobb, "TechSat21 – Space Missions Using Collaborating Constellations of Satellites," Proceedings of the *12th Annual AIAA/USU Conference on Small Satellites,* Logan, UT, August 1998, SSC98-VI-1.

[5] E. Olsen, *GPS Sensing for Formation Flying Vehicles*. Ph.D. Dissertation, Stanford University, Dept. of Aeronautics and Astronautics, Dec. 1999

[6] T. Corazzini, *Onboard Pseudolite Augmentation for Spacecraft Formation Flying*. Ph.D. Dissertation, Stanford University, Dept. of Aeronautics and Astronautics, Aug. 2000

[7] C. Park, *Precise Relative Navigation using Augmentd CDGPS*. Ph.D. Dissertation, Stanford University, Dept. of Mechanical Engineering, June. 2001

[8] G. F. Franklin, J. D. Powell, M. L. Workman *Digital Control of Dynamic Systems*. Addison-Wesley Inc., California, 1990.

[9] A. Gelb, *Applied Optimal Estimation*, MIT Press, Cambridge, MA, 1974

[10] T. Kailath, A. H. Sayed, B. Hassibi, *Linear Estimation* , Prentice Hall, Inc. Upper Saddle River, NJ, 2000

[11] M. H. Kaplan, *Modern Spacecraft Dynamics and Control*, John Wiley & Sons, Inc., 1976

[12] A. E. Bryson, *Dynamic Optimization*, Addison Wesley Longman, Inc., California, 1999.

[13] P. W. Binning, *Absolute and Relative Satellite to Satellite Navigation using GPS*. Ph.D. Dissertation, Dept. of Aerospace Engineering Sciences, University of Colorado, April 1997.

[14] J. R. Carpenter, D. C. Folta, D. A. Quinn NASA/Goddard Space Flight Center " Integration of Decentralized Linear-Quadratic-Gaussian Control into GSFC's Universal 3-D Autonomous Formation Flying Algorithm," Proceedings of the *AIAA Guidance Navigation and Control Conference,* Portland, OR, August 1999

[15] F. Gottifredi, L. Marradi, G. Adami, "Results from the ARP-GPS receiver Flight on the ORFEUS-SPAS Mission," *Proceedings of the ION-GPS Conference,*, Nashville, TN, Sept. 1999

[16] D. Gruenbacher, K. Strohbehn, L. Linstrom, B. Heins, G. T. Moore, and W. Devereux, "Design of a GPS Tracking ASIC for Space Applications," *Proceedings of the ION-GPS Conference*, Nashville, TN, Sept. 1999.

[17] R. Zenick and K. Kohlhepp, "GPS Micro Navigation and Communication System for Clusters of Micro and Nanosatellites," presented at the *Small Satellite Conference,* UT, Sept, 2000.

[18] K. Lau, S. Lichten, L. Young, "An Innovative Deep Space Application of GPS Technology for Formation Flying Spacecraft," *Proceedings of the American Institute of Aeronautics and Astronautics (AIAA) Guidance Navigation and Control Conference,* San Diego, CA, July 1996

[19] T. Corazzini and J. How, "Onboard Pseudolite Augmentation for Relative Navigation," *Proceedings of the ION-GPS Conference*, Nashville, TN, Sept 1999.

[20] J. C. Adams, *Robust GPS Attitude Determination for Spacecraft*. Ph.D. Dissertation, Stanford University, Dept. of Aeronautics and Astronautics, 1999

[21] E. Glenn Lightsey, *Development and Flight Demonstration of a GPS Receiver for Space*. Ph.D. Dissertation, Stanford University, Dept. of Aeronautics and Astronautics, Jan. 1997

[22] J. L. Speyer, "Computation and Transmisssion Requirements for a Decentralized Linear-Quadratic-Gaussian Control Problem," *IEEE Trans. Automatic Control,* vol. AC-24(2), 1979, pp.266-299.

[23] A. G.O. Mutambara *Decentralized Estimation and Control for Multisensor Systems*, CRC Press LLC, 1998

[24] S. H. Cobb, *GPS Pseudolites: Theory, Design, and Applications*. Ph.D. Dissertation, Stanford University, Dept. of Aeronautics and Astronautics, Dec. 1997